6-1-2013

β-Estradiol-dependent activation of the JAK/STAT pathway requires p/CIP and CARM1

N. Coughlan
Western University

G. Thillainadesan
Western University

J. Andrews
Western University, joseph.andrews@lhsc.on.ca

M. Isovic
Western University

J. Torchia
Western University

Biochimica et Biophysica Acta 1833 (2013) 1463–1475

Contents lists available at SciVerse ScienceDirect

Biochimica et Biophysica Acta

journal homepage: www.elsevier.com/locate/bbamcr

β-Estradiol-dependent activation of the JAK/STAT pathway requires p/CIP and CARM1

N. Coughlan [a,b,c], G. Thillainadesan [a,b,c], J. Andrews [a,b], M. Isovic [a,b], J. Torchia [a,b,c,*]

[a] Dept. of Oncology, The University of Western Ontario, Canada
[b] Dept. of Biochemistry, The University of Western Ontario, Canada
[c] London Regional Cancer Centre, Canada

ARTICLE INFO

Article history:
Received 17 August 2012
Received in revised form 15 January 2013
Accepted 11 February 2013
Available online 20 February 2013

Keywords:
Cancer
Estrogen
pCIP/CARM1
Coactivator
Chromatin

ABSTRACT

The steroid receptor coactivator p/CIP, also known as SRC-3, is an oncogene commonly amplified in breast and ovarian cancers. p/CIP is known to associate with coactivator arginine methyltransferase 1 (CARM1) on select estrogen responsive genes. We have shown, using a ChIP-on-chip approach, that in response to stimulation with 17β-estradiol (E2), the p/CIP/CARM1 complex is recruited to 204 proximal promoters in MCF-7 cells. Many of the complex target genes have been previously implicated in signaling pathways related to oncogenesis. Jak2, a member of the Jak/Stat signaling cascade, is one of the direct E2-dependent targets of the p/CIP/CARM1 complex. Following E2-treatment, histone modifications at the Jak2 promoter are reflective of a transcriptionally permissive gene, and modest changes in RNA and protein expression lead us to suggest that an additional factor(s) may be required for a more notable transcriptional and functional response. Bioinformatic examination of the 204 proximal promoter sequences of p/CIP/CARM1 targets supports the idea that transcription factor crosstalk is likely the favored mechanism of E2-dependent p/CIP/CARM1 complex recruitment. This data may have implications towards understanding the oncogenic role of p/CIP in breast cancer and ultimately allow for the identification of new prognostic indicators and/or viable therapeutic targets.

1. Introduction

Transcriptional activation is a highly dynamic process that involves a large and diverse class of proteins known as coactivators. Coactivators mediate specific transcriptional responses by utilizing several interrelated mechanisms involving chromatin remodeling and covalent modification of histones. These mechanisms often work cooperatively to alter the structural restrictions imposed by packaging DNA into chromatin. Additionally, many coactivators function as adaptors/bridging factors to recruit additional coactivator proteins to target genes [1]. Detailed genome-wide chromatin immunoprecipitation (ChIP) studies of binding sites for various transcription factors, such as the estrogen receptor (ER), have provided significant insight into the dynamics of coregulator activity at selected targets [2]. For example, the ER undergoes a cyclic pattern of association and dissociation at selected ER targets [2,12], and its association with DNA often coincides with the recruitment of several ERα-interacting complexes. These complexes consist of various combinations of coregulators, the basal transcriptional machinery, as well as RNA polymerase II [3]. The p/300 CBP interacting protein (p/CIP), also known as SRC3/AIB1/ACTR/RAC3, [4–9] belongs to a family of steroid receptor coactivator (SRC) proteins containing two additional family members (SRC1 and SRC2). p/CIP interacts directly with the liganded ER, and functions primarily as a bridging factor that binds to hormone-bound nuclear receptors to promote coactivator complex assembly [10,11]. ChIP assays have established that p/CIP associates with many endogenous ER target genes in response to 17β-estradiol (E2), including pS2 [3], cathepsin D [12] and cyclin D1 [13]. Additionally, p/CIP interacts with other liganded nuclear receptors [5,7–9] and other classes of transcription factors such as E2F [14] and NFkB [15].

Several studies have shown that p/CIP undergoes a variety of post-translational modifications in response to extracellular signals such as phosphorylation, acetylation, methylation, ubiquitination, and sumoylation [10,16–20]. These modifications provide an important regulatory mechanism that defines the combinatorial associations with additional coactivators, resulting in the formation of diverse multimeric complexes which generate distinct gene expression programs. The coactivator-associated arginine methyltransferase protein (CARM1) is one such coactivating partner that interacts with the carboxy terminus of p/CIP as well as other SRC proteins. CARM1 has been shown to methylate proteins involved in RNA processing as well as specific arginines at positions 17 and 26 on histone H3, suggesting that CARM1 plays a direct role in gene transcription [21,22]. Furthermore, several studies have demonstrated a correlation between recruitment of CARM1, methylation of histone H3, and activation of several steroid-responsive genes [23–26]. Sequential ChIP analysis has identified a

* Corresponding author at: Cancer Research Laboratories, London Regional Cancer Program, London, Ontario, Canada N6A 4L6. Tel.: +1 519 685 8692; fax: +1 519 685 8646.
E-mail address: jtorchia@uwo.ca (J. Torchia).

0167-4889/$ – see front matter.
http://dx.doi.org/10.1016/j.bbamcr.2013.02.009

complex consisting of p/CIP and CARM1 on several estrogen responsive genes [16,27,28], and CARM1 synergizes with p/CIP to activate NR-dependent transcription [29–31]. Collectively, these studies suggest that direct recruitment of CARM1 by p/CIP represents an essential activating step for ER-dependent transcription. In the present study, we have used sequential ChIP–reChIP assays in conjunction with genome-wide microarray screening to identify E2-dependent gene-promoter targets of the p/CIP/CARM1 complex. Importantly, our studies identify the JAK2 promoter as a novel target for the p/CIP/CARM1 complex in response to E2, indicating a novel interplay between ER signaling and the JAK/STAT pathway at the level of transcription, which may have implications in ER positive breast cancers where the JAK/STAT signaling pathway is constitutively active.

2. Results

2.1. Identification of genes directly targeted by the p/CIP/CARM1 complex in response to β-estradiol (E2)

To identify p/CIP/CARM1 target genes which play a role in E2-dependent signaling we embarked on a genome-wide chromatin immunoprecipitation assay approach based on *D*NA *S*election and *L*igation (ChIP-DSL) [32]. Briefly, MCF-7 cells were treated with E2 for 45 min and a standard ChIP assay was performed using an antibody against p/CIP. The immunoprecipitated material was then reChIPed using a CARM1-specific antibody. The resulting p/CIP/CARM1-enriched and input DNA was then purified, biotinylated, and combined with 20,000 unique predesigned oligonucleotides. After annealing, the biotinylated DNA was selected using streptavidin Sepharose and hybridized to a 20,000 gene promoter array (Fig. 1a). The identification of E2-dependent p/CIP/CARM1 targets was based on the following criteria: first, we established a list of genes displaying a statistically significant enrichment relative to input ($p<0.05$) regardless of the treatment. From this list, genes that displayed a 2-fold or greater enrichment in the E2-treated cells relative to control were identified (i.e. a twofold or greater enrichment was observed in cells treated with E2 as compared to the untreated cells). The experiment was performed in triplicate and based on these criteria we identified 204 gene promoters that become co-occupied by p/CIP and CARM1 in response to E2 treatment for 45 min (Fig. 1b–c & Table A1). To validate the ChIP-DSL analysis, we performed independent ChIP–reChIP experiments for a random set of target genes identified (Fig. 2). In the majority of cases tested, treatment with E2 resulted in the simultaneous recruitment of p/CIP and CARM1, indicating that the false positive rate was extremely low. It should be emphasized that in our experimental protocol we have identified gene targets for p/CIP/CARM1 as a consequence of E2 treatment; which may include genes directly regulated by the ER, as well as genes indirectly regulated by the ER through its association with other transcription factors, or via a nongenomic pathway.

2.2. The ER interacts with a fraction of p/CIP/CARM1 target gene promoters

To better validate our analysis, we compared our results with two previous studies examining direct E2-dependent ER binding on a genome-wide scale [33,34]. Carroll et al. discerned 3665 unique E2-dependent ER binding sites using a ChIP–chip Affymetrix Human tiling array approach [33], while Welboren et al. used a ChIP-Seq approach to identify 10,205 genome-wide ER-interaction sites [34]. Using the published chromosomal locations for ER-binding targets identified in these studies, we distinguished known genes present within and/or adjacent to these genomic sites. Next, we conducted direct gene-by-gene comparisons of p/CIP/CARM1 targets in our study with the ER targets identified in each of the previous studies. An important consideration for the purposes of this comparison is that while our analysis was restricted to the 1 kb proximal promoter regions of genes, the studies conducted by both the comparison groups encompassed binding sites throughout the entire genome. Notably, in each of studies used for comparative analysis, only a small proportion (4–7%) of ER-interaction sites were located within promoter regions. Nevertheless, our analysis indicated that 65/204 (32%) [33] and 118/204 (58%) [34] (Fig. 3a) of identified p/CIP/CARM1 complex targets have previously been shown to display ER binding following E2 treatment. Moreover, 59/204 (29%) p/CIP/CARM1 complex targets were ER binding targets common to both studies, and were therefore considered to be high confidence ER interactors (Fig. 3b, Table 1).

2.3. Binding site enrichment in the promoters of p/CIP/CARM target gene promoters

Since our p/CIP/CARM1 target genes may include genes directly and/or indirectly regulated by the ER, we examined 1 kb upstream promoter sequences of the gene targets for transcription factor binding site enrichment, to discern potential mechanisms for E2-dependent p/CIP/CARM1 binding. Using a candidate scanning approach, we conducted a search for enriched motifs within our target gene promoter sequences. Previous studies have shown that in addition to directly binding ER-binding elements (EREs) in response to ligand, the ER associates with C/EBP [35], and can also be targeted to the DNA via interaction with Oct [36,37], Sp1 [38,39] and/or AP-1 [40,41]. Forkhead motifs were also of interest, as evidence has linked the presence of the FoxA1/HNF3α motif to ER recruitment [33,42]. When p/CIP/CARM1 target gene promoter sequences were compared to a background control set of human housekeeping gene promoters, many enriched putative binding motifs were identified (Table A2). While EREs were shown as being significantly enriched among p/CIP/CARM1 complex promoters, it was not the most prevalent motif when ranked either by p-value or by enrichment score. Sp1, C/EBP, Oct, FoxA1, and AP-1 motifs were all found to be more significantly enriched than EREs among the p/CIP/CARM1 target gene promoters we identified. Evaluation of these consensus sites within the individual promoter sequences confirmed the presence and relative abundance of the motifs, with approximately 12% of target promoters containing one or more EREs, 31% C/EBPα motifs, 24% Sp1, 20% Oct, 10% FoxA1, and 9% contain putative AP-1 sites (Fig. 3c). Several of the promoters contain consensus sites for more than one of the considered transcription factors. EREs occurred simultaneously more often with C/EBP, Oct, and Sp1 motifs rather than with FoxA1 or AP-1 motifs (Fig. A1). While a negative correlation between ERE and AP-1 elements has previously been observed [33], our findings are contrary to previous reports [33,42] in that FoxA1 motifs did not consistently coincide with the presence of EREs. This discordance is likely due to our exclusive focus on the proximal promoter, since Kwon et al. also noted limited association of FoxA1 sites with proximal promoter ER binding events as identified by ChIP-DSL [43]. The overall enrichment pattern of putative transcription factor motifs did not change for the 59 p/CIP/CARM1 target genes that are considered to be high confidence ER binding targets (Fig. A2a) or for targets transcriptionally upregulated following E2 treatment (Fig. A2b).

Collectively, this analysis demonstrates a consistent pattern of enriched motifs among p/CIP/CARM1 complex target promoters, and suggests that transcription factor crosstalk is likely the favored mechanism of E2-dependent p/CIP/CARM1 recruitment at the proximal promoters of target genes, regardless of ER binding status or transcriptional state. The presence of EREs suggests that the classical response with direct binding of the ER is also involved, albeit to a lesser extent.

2.4. A proportion or p/CIP/CARM1 target genes are directly regulated by E2

To correlate p/CIP/CARM1 binding data with the E2-dependent transcriptional response, we performed gene expression profiling using MCF-7 cells treated with 10 nM E2 for 12 h. RNA was isolated, reverse transcribed and hybridized to Affymetrix microarrays. A list

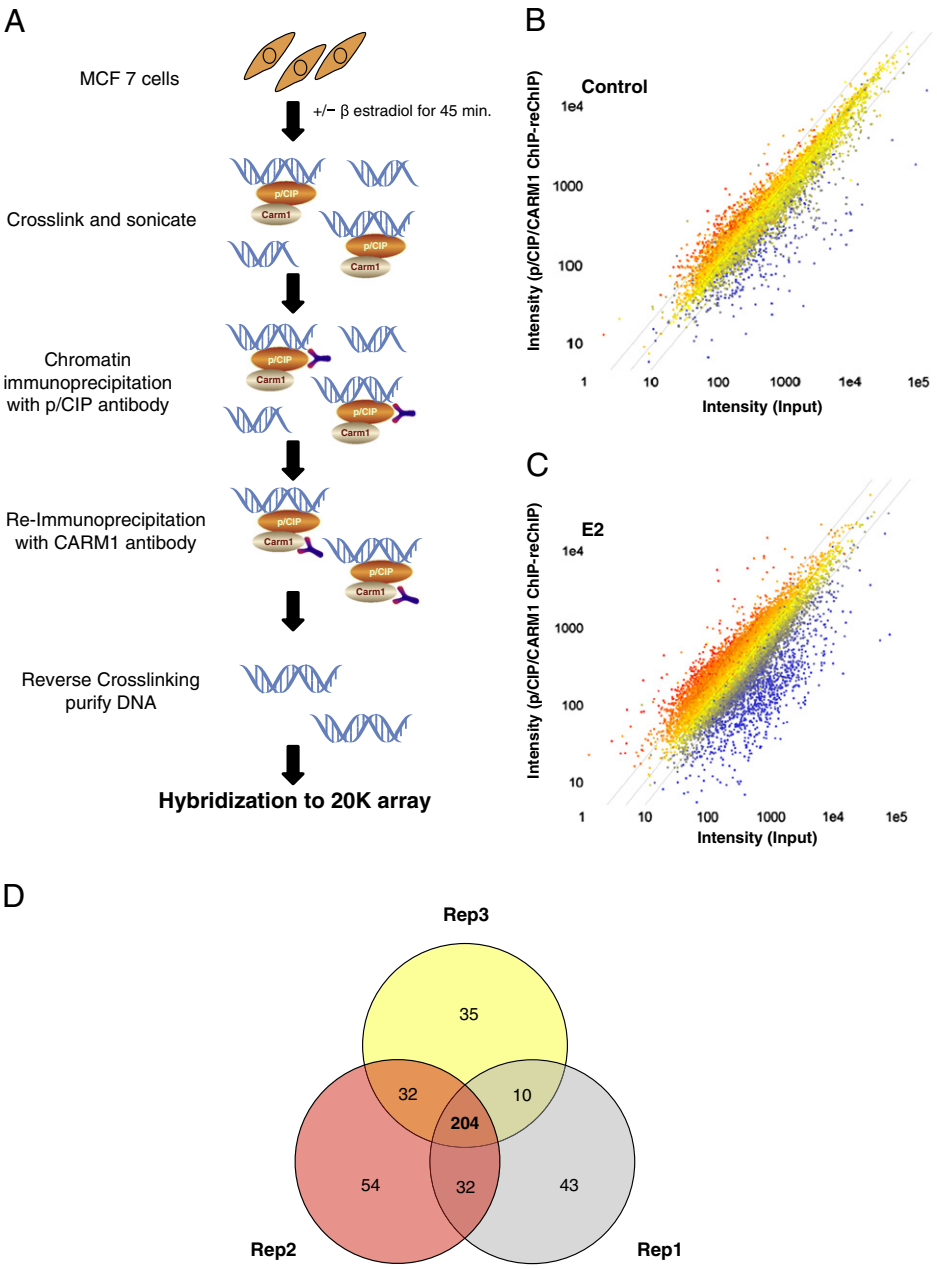

Fig. 1. ChIP-DSL analysis of p/CIP/CARM1 target genes in MCF-7 cells. (A) Sequential ChIP–reChIP coupled to DNA Selection and Ligation (ChIP-DSL) was used to assess global promoter occupancy by the p/CIP/CARM1 complex. Sequential ChIP–reChIP was performed using either IgG or anti-p/CIP followed by anti-CARM1 antibodies in control and 17β-estradiol stimulated MCF-7 cells. Total input and antibody-enriched DNA were biotinylated and annealed to a 40mer oligonucleotide pool. Annealed oligonucleotides were selected for with streptavidin-coated metal beads, and appropriate 40mers were ligated to form an 80mer, then labeled and hybridized to the Hu20K array, containing sequences from 20,000 unique human promoters. Scatter plots of (B) control and (C) 17β-estradiol stimulated p/CIP/CARM1 ChIP (y axis) versus input (x axis) from three independent biological replicates, demonstrating a normal cluster distribution. (D) Venn diagram depicting the overlap in genes enriched from three independent ChIP-DSL experiments (Rep 1 to 3).

of differentially expressed genes from three independent experiments was generated (p-value<0.05 was used as the cutoff). Based on this criteria, we identified 396 and 231 genes that were significantly upregulated or downregulated, respectively, following E2-treatment (Fig. 4a), consistent with previous expression profiling studies [43,44]. Comparison of the microarray expression data with the ChIP-DSL results determined that 33 (16.2%) targets proximally bound by the p/CIP/CARM1 complex are significantly upregulated, and 8 (3.9%) p/CIP/CARM1 target genes were downregulated following E2 treatment (Table 2). The reliability of this analysis was confirmed by quantitative real-time PCR (qPCR) analysis of selected genes (Fig. 4b). These findings suggests that proximal binding may be more relevant for transcriptionally upregulated genes, and shows that while the p/CIP/CARM1 complex may have a preferential role in transcriptional activation, it also plays a direct role in the repression of specific genes.

2.5. The JAK/STAT signaling pathway is a central target for p/CIP/CARM1

Using Ingenuity Pathway Analysis we were also able to identify a number of networks consisting of target genes that are functionally or biochemically linked. Several of the genes play a role in disease (Fig. 5a), and the molecular and cellular functions most associated with p/CIP/CARM1 target genes have been linked to the initiation and progression of cancer (Fig. 5b). We found that the network containing one of the highest number of functionally linked targets is the canonical JAK/STAT signaling pathway. Several interconnected

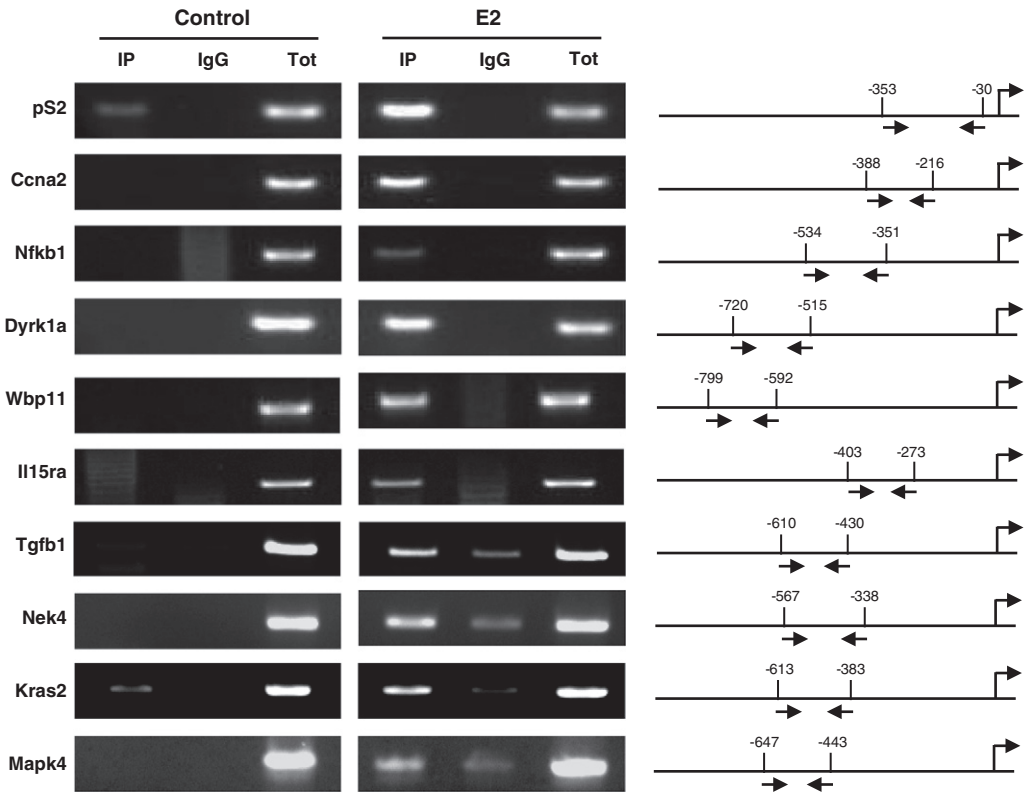

Fig. 2. ChIP analysis of selected direct p/CIP/CARM1 target genes. Control and 17β-estradiol stimulated MCF-7 cells were cross-linked with 1% formaldehyde, and sequential ChIP–reChIP was performed using either IgG or anti-p/CIP followed by anti-CARM1. Recovered DNA was assayed by PCR using primers corresponding to the promoter regions indicated. Selected target genes shown are pS2, Ccna2, Nfkb1, Dyrk1a, Wbp11, Il15ra, Tgfb1, Nek4, Kras2, and Mapk4.

genes within this pathway are direct targets for p/CIP and CARM1, including janus tyrosine kinase 2 (Jak2), the interleukin 15 receptor (Il15ra), and Pias2-a sumo ligase, which functions as a coregulator for STAT proteins (Fig. 4c, colored targets). Adding to the implied relevance of p/CIP/CARM1-mediated regulation of this pathway, Stat3 and Stat5 (Fig. 4c, gray targets) were also identified as E2-dependent p/CIP/CARM1 binding targets, however, they were not included on the final list as they did not meet the applied statistical criteria. We focused our initial analysis on the Jak2 gene. JAK2 plays a central role in JAK/STAT signaling and mammary gland development, and hyperactivation of this protein is associated with cancer initiation. Importantly, functional ablation of JAK2 in mice protects against the onset of mammary tumorigenesis [45].

2.6. E2-dependent regulation of JAK2

JAK2 expression was assessed using qPCR following E2 treatment of MCF-7 cells for various time periods. We observed an initial decrease in Jak2 expression 1 h following E2 treatment, and a gradual increase in expression thereafter, such that at 12 and 24 h the expression levels are consistent with preliminary expression array data, with an approximately 1.5-fold increase in expression when compared to the untreated control ($p<0.05$) (Fig. 4b). Analysis of JAK2 protein levels exhibit a corresponding trend, with a modest increase (~1.3 fold) in protein expression after 12 and 24 h of E2 stimulation, followed by a decrease to control unstimulated expression levels at 72 h (Fig. 4d).

To validate recruitment of p/CIP and CARM1 to specific regions of the Jak2 promoter we performed ChIP assays. For the purposes of this analysis, we used a region of the promoter that corresponds to a region 787 to 950 bp upstream of the transcriptional start site (TSS) (Fig. 6a). An ERE-Sp1 half-site was identified within this portion of the Jak2 promoter.

Cells were treated with E2 for 45 min and promoter occupancy was assessed by sequential ChIP assay using specific antibodies recognizing p/CIP and CARM1. In addition, ChIP assays were performed using an antibody against the ER to assess a possible mechanism of recruitment for the p/CIP/CARM1 complex to the Jak2 promoter. We found that the p/CIP/CARM1 complex binds in a ligand-dependent manner to the Jak2 promoter (Fig. 6b). Importantly, we also determined that the ER also binds Jak2 in response to ligand (Fig. 6b). The presence of both the p/CIP/CARM1 complex and the ER at the same region of the promoter suggests that E2-dependent complex recruitment to the Jak2 promoter is mediated through its interaction with the ERE-associated ER. This finding is consistent with the putative status of Jak2 as one of the 59 high-confidence ER targets.

To determine whether the E2-dependent assembly of a p/CIP/CARM1 complex impacts the chromatin marks at the Jak2 promoter, ChIP analysis was performed using antibodies corresponding to histone modifications associated with transcriptional status; histone H3 lysine 4 trimethylation (H3K4me3) and acetylation of histone H3 at Lysines 9 and 14 (H3Ac) are modifications generally indicative of transcriptionally active chromatin structure [46,47]. In addition, CARM1 is known to asymmetrically dimethylate arginine 17 on histone H3 (H3R17me2), a mark that is also associated with transcriptional activation [48].

E2-dependent changes in histone modifications were observed at the Jak2 promoter. In response to treatment, there was a modest increase in acetylation of H3K9 and H3K14 (H3K9/14ac) (Fig. 6c) and a statistically significant enrichment in dimethylation of H3R17me (Fig. 6d), consistent with recruitment of a functional p/CIP/CARM1 complex. Surprisingly, trimethylation of H3K4 remained unchanged by E2 treatment (Fig. 6c), perhaps suggestive of a transcriptionally permissive but not fully active gene state, in agreement with modest E2-dependent increases in mRNA observed (Fig. 4b).

To determine if the changes in histone modifications are dependent on the presence of p/CIP, quantitative ChIP analysis was performed on

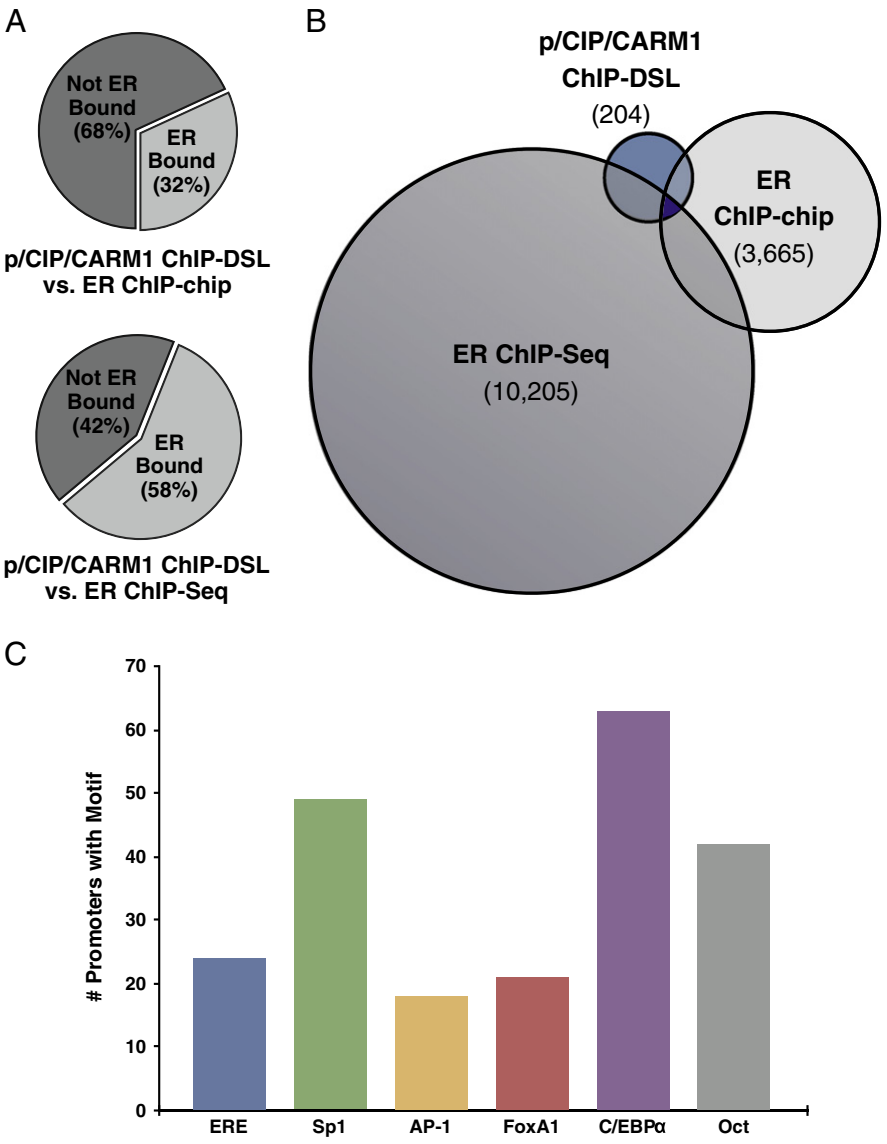

Fig. 3. Binding site enrichment analysis of p/CIP/CARM1 target promoter sequences. (A) Pie charts indicating the proportion of p/CIP/CARM1 target genes that are known to bind the ER based on comparison with ChIP–chip analysis performed by Carroll et al. (top) and ChIP-Seq analysis performed by Welboren et al. (bottom). (B) Venn diagram showing overlap of p/CIP/CARM1 direct target genes (highlighted in blue) with ER-binding sites identified by ChIP–chip reported by Caroll et al. and identified by ChIP-Seq reported by Welboren et al. 59 p/CIP/CARM1 target genes were common to both the Carroll et al. and Welboren et al. analysis, and were considered to be high confidence ER-binding targets. (C) Bar graph showing the number of individual p/CIP/CARM1 target promoters that contain ERE, Sp1, AP-1, FoxA1, C/EBP, and Oct binding motifs.

the Jak2 promoter following siRNA-mediated gene silencing of p/CIP. p/CIP was present minimally on the promoter despite p/CIP depletion (Fig. 7b), likely due to incomplete knockdown (Fig. 7a). The level of p/CIP present on the promoter was increased in response to hormone (Fig. 7b). The functional effect of p/CIP depletion was determined by ChIP assay evaluating the presence of the CARM1-dependent histone modification H3R17me2 in response to E2. As a chromatin mark associated with transcriptional activation, in the absence of p/CIP [and complex] recruitment, E2-dependent dimethylation of R17 on histone H3 was reduced (Fig. 7b), indicating that p/CIP is likely required for recruitment of CARM1, and its subsequent methyltransferase activity.

To further our understanding of the role that the p/CIP/CARM1 complex plays in regulating Jak2, we assessed its E2-dependent expression in the absence of p/CIP or CARM1. When a control siRNA was used, we saw a statistically significant induction of Jak2 expression, based on realtime PCR, after 12 and 24 h of E2 treatment. However, when p/CIP was downregulated using siRNA, this effect was diminished (Fig. 7c). A similar experiment was performed following CARM1 knockdown and, although the knockdown was not complete, there was a more dramatic loss of E2-dependent Jak2 expression as compared to p/CIP knockdown (Fig. 7d). Interestingly, when MCF7 cells were treated with E2, we also observed an increase in Stat3 phosphorylation, indicative of E2-dependent JAK/STAT pathway activation. However, when either p/CIP or CARM1 was depleted, this effect was lost (Fig. 7c–d). Collectively, this data suggests that p/CIP and CARM1 are in part required for the E2-dependent regulation of Jak2 transcription and activation of the JAK/STAT signaling pathway in MCF7 cells.

3. Discussion

In the present study, we identified E2-dependent target genes for the p/CIP/CARM1 coregulatory complex. We then determined the transcriptional status of those genes following 12 h E2 treatment, and compared the lists with known ER binding sites in an attempt to clarify a mechanism for complex recruitment and subsequent gene regulation.

Global characterization of p/CIP (SRC-3) binding sites conducted by Lanz et al. identified 12,294 E2-dependent targets using ChIP-Seq, 5512

Table 1
p/CIP/CARM1 target genes bind the ER.

Gene ID	Accession number	Description
TLR3	NM_003265	Transmembrane receptor
DBC1	NM_014618	Peptidase
LAP3	NM_015907	Peptidase
CLDN12	NM_012129	Calcium-independent cell–cell adhesion
SLC4A5	NM_021196	Solute carrier family 4, sodium bicarbonate cotransporter, member 5
PTER	NM_030664	Phosphotriesterase related
TRAF3	NM_003300	TNF receptor-associated factor 3/apoptosis
LETM1	NM_012318	Leucine zipper-EF-hand containing transmembrane protein 1
IGSF4/CADM1	NM_014333	Cell adhesion molecule 1/tumor suppressor
OCA2	NM_000275	Oculocutaneous albinism II
SLC26A1	NM_022042	Solute carrier family 26 (sulfate transporter), member 1
FRMD1	NM_024919	FERM domain containing 1
N4BP1	NM_153029	NEDD4 binding protein 1
CTNND1	NM_001331	Catenin (cadherin-associated protein), delta 1
CDH7	NM_033646	Cadherin 7, type 2
RAD9B	NM_152442	RAD9 homolog B (*S. cerevisiae*)/DNA replication
ECT2	NM_018098	Epithelial cell transforming sequence 2 oncogene
PCSK5	NM_006200	Proprotein convertase subtilisin/kexin type 5
GATM	NM_001482	Glycine amidinotransferase (L-arginine:glycine amidinotransferase)
TUBGCP6	NM_020461	Tubulin, gamma complex associated protein 6
KCTD16	XM_098368	Potassium channel tetramerization domain containing 16
TGFB1	NM_000660	Growth factor
NEK4	NM_003157	Enzyme
RPS4X	NM_001007	Ribosomal protein S4, X-linked
STARD4	NM_139164	StAR-related lipid transfer (START) domain containing 4
HRASLS	NM_020386	HRAS-like suppressor
PKP4	NM_003628	Plakophilin 4/cell adhesion
SMARCAL1	NM_014140	SWI/SNF related, matrix associated, regulator of chromatin, a-like 1
CD9	NM_001769	CD9 molecule/cell adhesion
C9orf95	NM_017881	Orf
TMEM16F	XM_113743	Transmembrane protein 16 F
IVNS1ABP	NM_006469	Influenza virus NS1A binding protein
DDX54	NM_024072	DEAD (Asp-Glu-Ala-Asp) box polypeptide 54/transcriptional regulator
ITPKB	NM_002221	Inositol 1,4,5-trisphosphate 3-kinase B
POLR2F	NM_021974	Polymerase (RNA) II (DNA directed) polypeptide F
LAMA1	NM_005559	Laminin, alpha 1/cell adhesion protein
TSHB	NM_000549	Thyroid stimulating hormone, beta
RDH10	NM_172037	Retinol dehydrogenase 10 (all-trans)
KCNQ1	NM_000218	Potassium voltage-gated channel, KQT-like subfamily, member 1
KCTD3	NM_016121	Potassium channel tetramerization domain containing 3
PCP4	NM_006198	Purkinje cell protein 4
LRFN4	NM_024036	Leucine rich repeat and fibronectin type III domain containing 4
ABAT	NM_000663	4-aminobutyrate aminotransferase
PTPRJ	NM_002843	Protein tyrosine phosphatase, receptor type, J
JAK2	NM_004972	Janus kinase 2 (a protein tyrosine kinase)
GPR132	NM_013345	G protein-coupled receptor 132
HARS	NM_002109	Histidyl-tRNA synthetase
MDS009	NM_020234	DTWD1 DTW domain containing 1
POLG	NM_002693	Polymerase (DNA directed), gamma
HSD17B12	NM_016142	Hydroxysteroid (17-beta) dehydrogenase 12
AKAP13	NM_006738	A kinase (PRKA) anchor protein 13
DPYS	NM_001385	Dihydropyrimidinase
DYRK1A	NM_101395	Dual-specificity tyrosine-(Y)-phosphorylation regulated kinase 1A
EDC3	NM_025083	Homo sapiens enhancer of mRNA decapping 3 homolog (*S. cerevisiae*)
SLC39A10	XM_047707	Solute carrier family 39 (zinc transporter), member 10
SAMD3	NM_152552	Sterile alpha motif domain containing 3
FLRT2	NM_013231	Fibronectin leucine rich transmembrane protein 2/cell adhesion
MGC14156	NM_032906	PIGY phosphatidylinositol glycan anchor biosynthesis, class Y
MXD3	NM_031300	MAX dimerization protein 3

of which were distinct from those found using vehicle stimulation [49]. Many of these sites overlap with previously identified ER binding regions, and, in accordance with accumulating genomic analysis indicating that the majority of ER binding sites are located in regions far upstream of the TSS, only a minority (~3%) of E2-dependent p/CIP binding is suggested to occur within 500 bp of the TSS. The level of CARM1 activity (as assayed by its methylation of H3R17 and/or p/CIP) across the genome also appears to cluster predominantly at a distance from promoters [50]. These observations of a limited set of proximal promoter binding sites for p/CIP, and minimal CARM1 methylation activity at promoter elements correspond with the relatively small number of promoters we identified as interacting with the p/CIP/CARM1 complex, and is also consistent with proximal ER binding events previously identified using the 1 kb promoter-specific ChIP-DSL approach [43]. Although now largely superseded by ChiP-Seq, ChIP-DSL is a highly sensitive assay which eliminates some of the biases introduced by more conventional ChIP-on-chip whole-genome approaches. In ChIP-DSL, the immunoprecipitated genomic DNA is used only as a template to mediate annealing and ligation of aligned oligonucleotide pairs. After annealing, the biotinylated DNA is then selected using streptavidin Sepharose and Taq ligase is used to ligate oligonucleotides positioned directly adjacent to each other, creating complete amplicons which are hybridized to a 20,000 gene promoter array. A limitation of this approach is that analysis is restricted to those promoters found on the

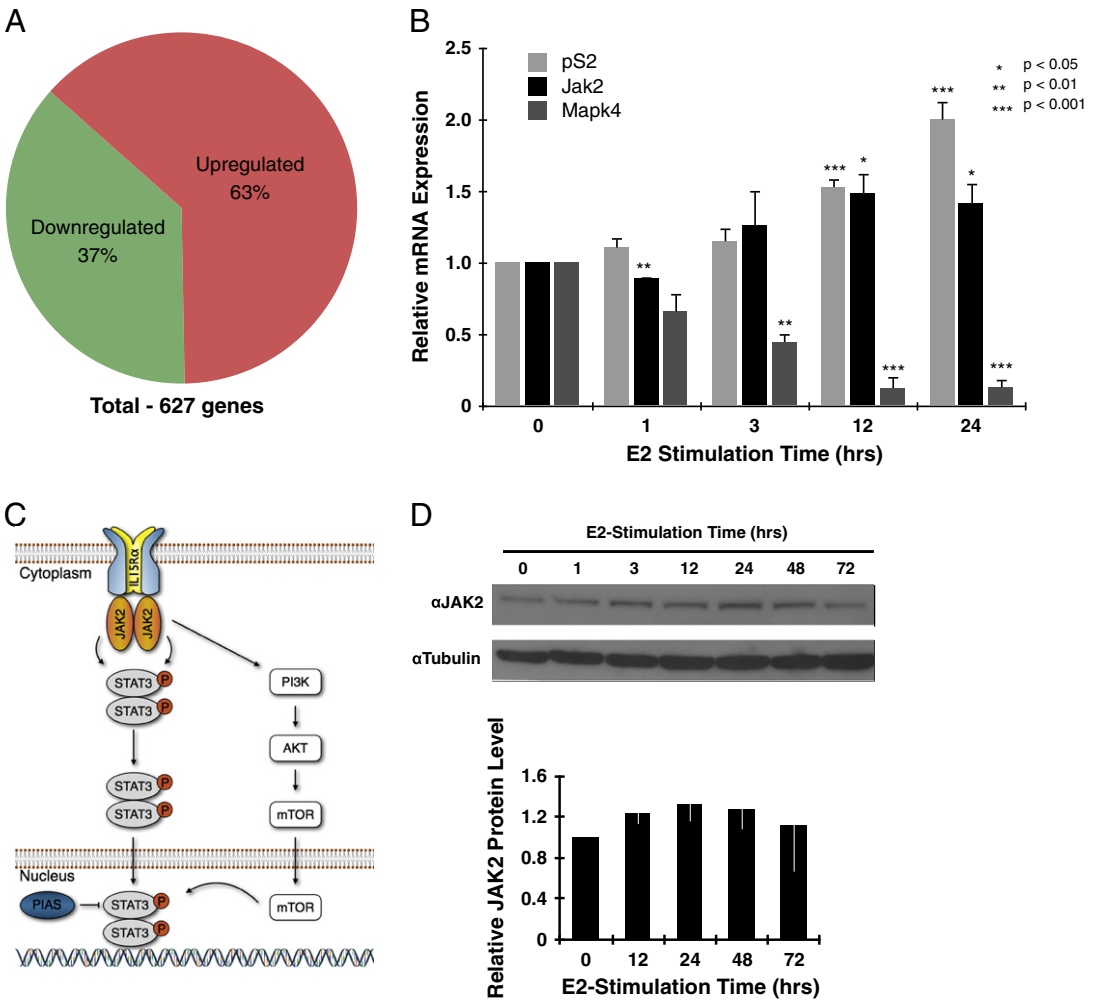

Fig. 4. p/CIP/CARM1 target genes are directly regulated by E2. (A) Differentially expressed genes after E2-stimulation relative to unstimulated control cells. (B) Realtime RT-PCR analysis of pS2, Jak2, and Mapk4 following stimulation of MCF-7 cells with 17β-estradiol for 1 h, 3 h, 12 h, and 24 h. Data is expressed as means and standard error of the mean from repeated experiments, performed independently (pS2 n = 7, Jak2 n = 7, Mapk4 n = 3). Paired student's *t*-test was performed and statistically significant changes from untreated samples are indicated. (C) Canonical pathway diagram, highlighting statistically significant p/CIP/CARM1 complex direct targets in color. Targets in gray are bound by p/CIP/CARM1 but do not meet statistical criteria. (D) Western blot showing JAK2 levels in MCF7 cells following 17β-estradiol stimulation of MCF7 cells for 1, 3, 12, 24, 48, and 72 h. Relative abundance of protein levels at 12, 24, 48, and 72 h time points was quantified by densitometry.

array which contain 1 kb of upstream regulatory sequence. Studies have shown that the majority of ER binding sites are found more distal than the proximal promoter. Nevertheless, promoter proximal interactions do occur in response to E2 and this interaction can have transcriptional consequences. Furthermore, our study does not examine ER binding directly, but rather focuses on occupancy of p/CIP/CARM1 in response to E2. Thus, it would theoretically include those targets that are targeted to promoter regions by E2 independent of direct DNA binding, and possibly via enhancer–promoter interactions.

A major advantage of this approach is that we identified 204 promoter-proximal interaction sites for the p/CIP/CARM1 complex, eliminating the complicated process of assigning responsive genes to distant binding sites, and instead were able to directly correlate complex interaction with transcriptional effect. Previous microarray studies with E2-stimulation can be broadly categorized based on the length of hormone treatment. There is an observable difference in the pattern of expression change, such that at early time points (<6 h) more genes are upregulated and more variation is evident between time points, while at later time points (>12 h) there is a more stable pattern of expression change and the majority of genes are downregulated [33,44]. We showed that after 12 h of stimulation with E2, 20% of p/CIP/CARM1 complex target genes identified by ChIP-DSL were transcriptionally altered (16.2% upregulated and 3.9% downregulated). The relatively small number of transcriptionally changed target genes after 12 h implies that proximal recruitment of the p/CIP/CARM1 complex is not predictive of E2-dependent gene expression at this late time point. However, among those targets that are transcriptionally altered, the complex plays a preferential role in activation, consistent with the role of p/CIP as a coactivator. While the changes in target gene expression that we observed were modest, we do observe notable changes in chromatin modifications, suggesting that E2 may facilitate crosstalk.

Direct comparison of target gene promoters in our study with known genomic ER binding sites in MCF-7 cells [under equivalent E2-stimulation conditions] [33,34] identified 59/204 (29%) p/CIP/CARM1 complex targets as putative high-confidence ER binding targets. Therefore, it seems likely that the p/CIP/CARM1 complex is recruited to this subset of E2-responsive promoters via the ER. We also identified a trend in which binding motifs for transcription factors known to facilitate ER recruitment were enriched among p/CIP/CARM1 complex target promoter sequences. While Sp1, C/EBP, Oct, FoxA1, and AP-1 motifs have previously been shown to be enriched, in addition to EREs, in the sequences surrounding ER binding events on a genome-wide scale [33,42,50], there has not previously been much discussion related to the proximal promoter region or when considering recruitment of an E2-regulated complex. Neither the predicted ER-binding state nor the transcriptional status of complex target genes after 12 h E2 treatment

Table 2
Genes directly regulated by the p/CIP/CARM1 complex[a].

Gene ID	Accession number	Description
Genes activated by E2		
NFKB1	NM_003998	Nuclear factor of kappa light polypeptide gene enhancer
MOCOS	NM_017947	Enzyme
JAK2	NM_004972	Janus kinase 2 (a protein tyrosine kinase)
STARD4	NM_139164	StAR-related lipid transfer (START) domain containing 4
HARS	NM_002109	Histidyl-tRNA synthetase
IGSF4/ CADM1	NM_014333	Cell adhesion molecule 1/tumor suppressor
KCTD3	NM_016121	Potassium channel tetramerization domain containing 3
GTF2E2	NM_002095	General transcription factor IIE, polypeptide 2, beta 34 kDa
ZIM3	NM_052882	Zinc finger, imprinted 3/transcription factor
PDCD8	NM_004208	Enzyme/cell death
WBP11	NM_016312	WW domain binding protein 11
PRKRIR	NM_004705	Protein-kinase, interferon-inducible RNA dependent inhibitor
ZNF567	NM_152603	Transcription factor
IVNS1ABP	NM_006469	Influenza virus NS1A binding protein
BMI1	NM_005180	BMI1 polycomb ring finger oncogene
M6PR	NM_002355	Mannose-6-phosphate receptor (cation dependent)
HSD17B12	NM_016142	Hydroxysteroid (17-beta) dehydrogenase 12
TM4SF8	NM_005724	Tetraspanin 3
CCNA2	NM_001237	Cyclin A2/cell cycle
LAP3	NM_015907	Peptidase
POLR2F	NM_021974	Polymerase (RNA) II (DNA directed) polypeptide F
RAD9B	NM_152442	RAD9 homolog B (*S. cerevisiae*)/DNA replication
DYRK1A	NM_101395	Dual-specificity tyrosine(Y)-phosphorylation regulated kinase 1A
PCNA	NM_002592	Proliferating cell nuclear antigen
PCP4	NM_006198	Purkinje cell protein 4
ZNF800	NM_176814	Unknown
PELO	NM_015946	Pelota homolog (*Drosophila*)
DPH2L2	NM_001384	DPH2 homolog (*S. cerevisiae*)
RFXAP	NM_000538	Regulatory factor X-associated protein
CLDN12	NM_012129	Calcium-independent cell–cell adhesion
PIAS2	NM_004671	Protein inhibitor of activated STAT, 2
ELAC1	NM_018696	ElaC homolog 1 (*E. coli*)/trna processing
RDH10	NM_172037	Retinol dehydrogenase 10 (all-trans)
Genes repressed by E2		
PXMP4	NM_007238	Peroxisomal membrane protein 4, 24 kDa
HBD	NM_000519	Hemoglobin, beta///hemoglobin, delta
MAPK4	NM_002747	Mitogen-activated protein kinase 4
ITPKB	NM_002221	Inositol 1,4,5-trisphosphate 3-kinase B
MXD3	NM_031300	MAX dimerization protein 3
MGC15882	NM_032884	C1orf94
LMOD1	NM_012134	Leiomodin 1 (smooth muscle)
CD9	NM_001769	CD9 molecule/cell adhesion

[a] Comparative analysis of ChIP–chip data and expression analysis following 12 h E2-stimulation of MCF-7 cells allowed for the identification of p/CIP/CARM1 regulated genes.

was predictive of enrichment of transcription factor binding motifs studied, and so, consensus mechanisms for differential transcriptional responses as implied by the recruitment of the ER could not be inferred.

Several of the targets identified are components of the canonical JAK/STAT signaling pathway. This pathway mediates the activity of a wide variety of cytokines and growth factors [51]. JAK2 is a central component of the pathway and is responsible for phosphorylation and activation of the STAT family of proteins, which normally reside in the cytoplasm and, upon activation, translocate to the nucleus and bind to specific target genes involved in cell proliferation and survival [51]. JAK2 or STAT5 null mice display phenotypes remarkably similar to the ERα and p/CIP knockout animals including defects in mammary gland cell proliferation and apoptosis [52,53]. Importantly, overexpression or constitutive activation of STAT3 and 5 proteins has been described in many types of cancers [54] and promote the occurrence of sporadic mammary cancers in mice [45,55–57]. In proliferating ER-positive tumor cells, E2 is known to stimulate phosphorylation and activation of STAT3 and 5, although the mechanism has not been fully elucidated [58–60]. The PIAS family, most notably recognized for their role as coregulators for STAT proteins, is also of interest as PIAS1 has been shown to sumoylate p/CIP [and other SRCs], affecting activity and stability in steroid-receptor signaling pathways in MCF7 cells [20]. Collectively, these findings suggest that ER signaling and the JAK/STAT pathway may cooperate in the regulation of mechanisms implicated in mammary cancers. This cooperation may be mediated, at least in part, through the p/CIP/CARM1 complex.

We observed recruitment of the p/CIP/CARM1 complex to the 1 kb promoter of Jak2 in response to E2, with a transcriptional upregulation after 12 and 24 h, but no significant effect on protein levels with E2 stimulation. Analysis of histone modifications to the proximal 1 kb promoter revealed an unclear pattern that was predictive neither of transcriptional activation nor repression. A modest increase in acetylation of histone H3 at K9 and K14 at a region approximately 1 kb upstream of the Jak2 TSS in response to E2, which coincides with p/CIP/CARM1 complex recruitment, suggestive of a transcriptionally active gene. In contrast, there was a lack of discernible change in H3K4me3 in response to E2 at the same promoter region, a modification that would be expected to be present near the TSS of an actively transcribed gene [61,62]. We suggest that these changes reflect a promoter that is not necessarily in line with a fully transcriptionally active state but may instead be permissive, poised for more robust transcriptional activation, in a process that may require additional signals.

Our study of chromatin modifications was focused to a single time point for E2 treatment. This is based on previous studies showing maximal p/CIP/CARM1 recruitment to the pS2 promoter 45 min after the addition of hormone [16]. Importantly, a statistically significant E2-dependent increase in H3R17me2 was evident, corresponding with the region of p/CIP/CARM1 recruitment, suggesting the complex is functional on the Jak2 promoter. Reinforcing this idea, we noted that following depletion of p/CIP, E2-dependent H3R17me2 of the Jak2 promoter was greatly reduced in addition to an observable loss of p/CIP recruitment. Finally, siRNA mediated depletion of p/CIP resulted in a reduction in E2-induced transcription of Jak2, with residual E2-responsiveness likely due to functional redundancy between SRC family members. However, depletion of CARM1 caused a more dramatic loss in E2-dependent Jak2 transcription, suggesting that its enzymatic activity is in fact important for the observed regulation by the p/CIP/CARM1 complex. CARM1 activity has previously been associated with the regulation of a subset of the ER cistrome [50], and herein we provide a specific example of its E2-dependent recruitment, as part of an active coregulatory complex, to the Jak2 promoter. We also observed an increase in phosphorylated STAT3, indicative of activation of the JAK/STAT signaling pathway. While this activation is not necessarily dependent on Jak2 transcriptional upregulation, this effect was lost following siRNA-mediated silencing of p/CIP or CARM1.

Collectively, while the changes in E2-dependent H3R17 dimethylation are indicative of active Jak2 transcription, the other chromatin marks we examined, as well as the modest response at the RNA and protein levels, were inconsistent with a fully transcriptionally active promoter. We suggest that an additional signal may be required for a more robust transcriptional response of the Jak2 gene. In addition, despite the changes in expression of select genes, the majority of complex targets did not exhibit a widespread transcriptional response to 12 h E2 treatment, ultimately suggesting that E2 may cause a general “rewiring” of specific signaling pathways, through recruitment of the p/CIP/CARM1 complex, so that many essential genes become “poised” for transcription.

4. Materials and methods

4.1. Plasmids, antibodies, and reagents

A complete list of primers used can be found in Table A3 of the supplemental material. Antibodies used in this study are listed in

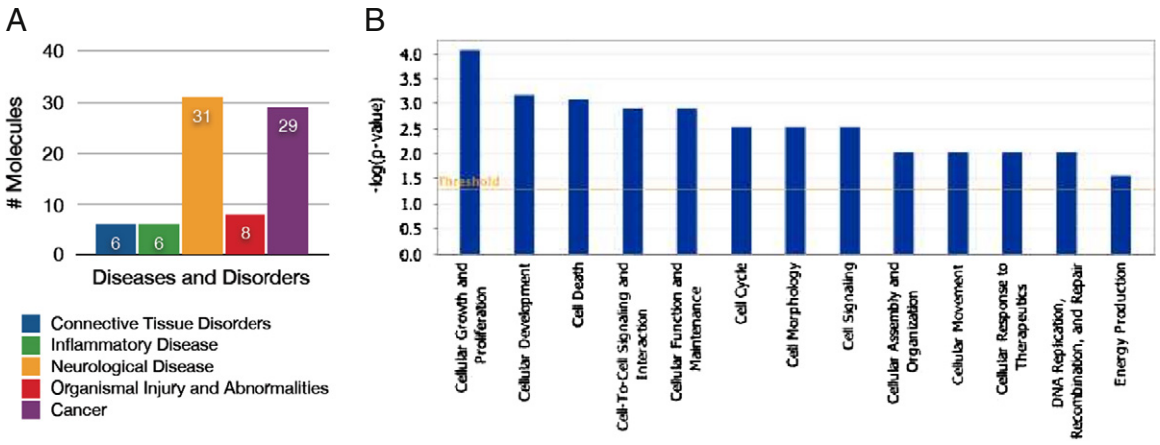

Fig. 5. Functional classification of p/CIP/CARM1 target gene promoters. (A) Schematic Ingenuity Pathway Analysis indicates (A) that cancer is one of the diseases most commonly associated with the p/CIP/CARM1 target genes and (B) that molecular and cellular functions associated with the gene set highlight cellular growth and proliferation as predominating.
Adapted from © 2000–2011 Ingenuity Systems, Inc. All rights reserved.

Table A4 of the supplemental material. All of the antibodies used for these studies are commercial antibodies, with the exception of the p/CIP antibody. The method by which this antibody was generated, purified, and tested has been previously described [4]. 17β-Estradiol (water soluble) was purchased from Wisent. All siRNA used was purchased from Dharmacon.

4.2. Western blotting

Cells were grown in phenol red-free, charcoal stripped DMEM and stimulated with 10^{-7} M E2 for various time periods as indicated. Cells were washed twice in phosphate buffered saline (PBS), harvested and lysed in RIPA lysis buffer (~150 μl/60 mm plate) consisting of 50 mM

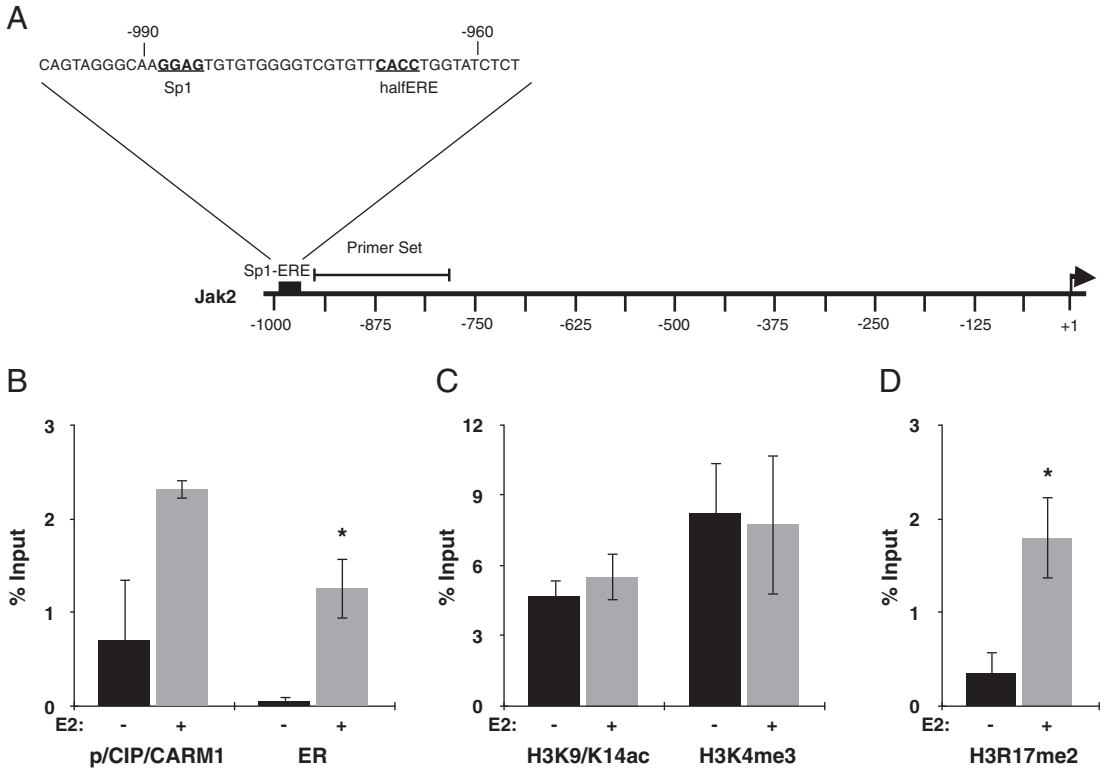

Fig. 6. Characterizing E2-dependent histone modifications to Jak2 proximal promoter. (A) Schematic representation of the Jak2 1 kb proximal promoter, highlighting region used for ChIP analysis. (B) Control and 17β-estradiol stimulated MCF-7 cells were cross-linked with 1% formaldehyde, and ChIP or sequential ChIP–reChIP was performed using the indicated antibodies, followed by qPCR. ChIPs were performed in triplicate, normalized to IgG, and shown as percentage of Input. Statistical significance was determined using Student's *t*-test and is indicated by * ($p<0.05$). (C–D) ChIP-qPCR analysis of Jak2 promoter following E2 treatment. ChIPs were performed in duplicate (H3K9/k14ac, H3K4me3) or triplicate (H3R17me2) using indicated antibodies, quantitated with real-time PCR, normalized to IgG control and shown as percentage of Input. Statistical significance was determined using Student's *t*-test and is indicated by * ($p<0.05$).

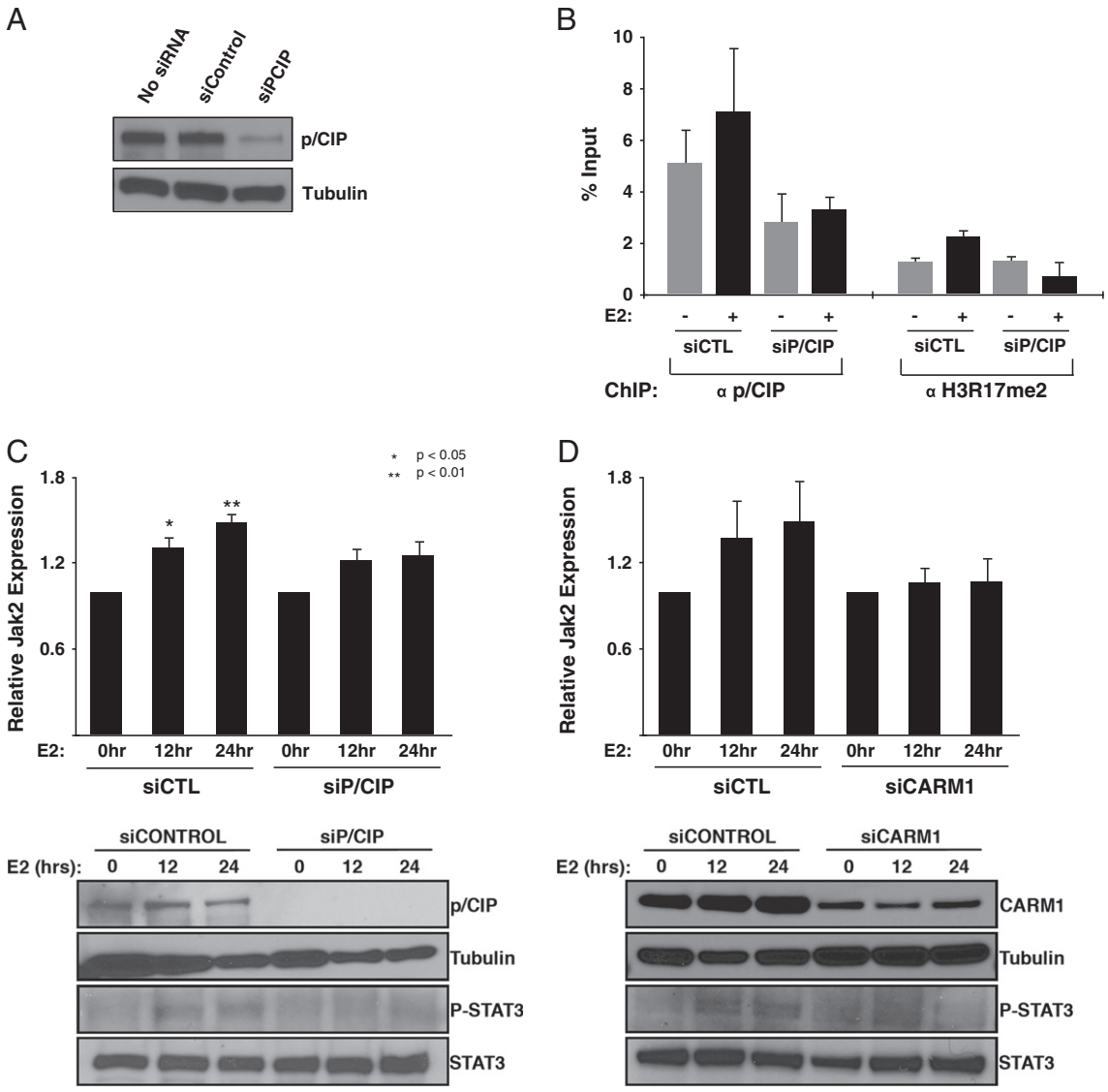

Fig. 7. p/CIP/CARM1 mediated E2-dependent regulation of Jak2. (A) Representative Western blot showing 72 h siRNA depletion of p/CIP in MCF7 cells. (B) ChIPs were performed in triplicate at Jak2 promoter regions using indicated antibodies, quantitated by real-time PCR, normalized to IgG control and shown as a percentage of Input. Data is expressed as means and standard error of the mean from triplicate experiments. (C–D) Analysis of E2-dependent Jak2 transcription (top) and STAT3 activation (bottom) with siRNA-mediated depletion of (C) p/CIP or (D) CARM1. (Top) Realtime RT-PCR analysis of Jak2 was performed following 12 and 24 h exposure to hormone, and data is expressed as the mean and standard error of the mean from triplicate experiments, performed independently. Student's *t*-test was used to compare E2-induced expression changes and statistically significant differences from control samples are indicated. (Bottom) Representative Western blot showing knockdown efficiency and STAT3 activation in MCF7 cells following E2 treatment.

Tris (pH 8.0), 150 mM NaCl, and 1% NP-40, 0.1% SDS and protease inhibitor cocktail. Extracts were centrifuged for 10 min at 14,000 rpm at 4 °C and the soluble fractions were retained. Samples were normalized for protein content and were separated by SDS-PAGE, transferred to nitrocellulose or PVDF membrane and blocked overnight in PBS containing 0.1% TWEEN-20 and 5% nonfat dried milk. The appropriate antibodies were then diluted in blocking buffer and the membrane was probed for 2 h at room temperature with rocking, followed by incubation with secondary antibody for 1 h. Proteins were detected using ECL according to the manufacturer's recommendations (Amersham).

4.3. RNA isolation and real-time PCR

Total cellular RNA was isolated using RNeasy kit (Qiagen). The quality and quantity of RNA were evaluated by measuring OD 260/280. For real-time PCR analysis, 0.2 μg of RNA was reverse-transcribed with TaqMan reverse transcriptase (Applied Biosystems) using random hexamers to generate cDNA. All amplicons were detected using the 5′ nuclease (Taqman) assay with 5′ labeled probes. Probes were already predesigned and quality tested (Applied Biosystems). Reactions were performed according to the manufacturer's recommendations (Applied Biosystems) and were run in replicates of two, in a 96-well format. Each reaction included 18S RNA as a control for normalization, and reactions lacking cDNA served as negative controls. Two independent experiments were performed for each gene following treatment with E2, and a mean value was obtained and compared to the mean expression level of each gene from untreated cells. Applied Biosystems 7500 Real Time PCR System software was used to identify cycle threshold (Ct) for each reaction.

4.4. RNA microarray analysis

Total RNA was extracted from MCF-7 cells treated with 10 nM E2 for 12 h and from control, untreated cells. Independent biological triplicates were performed for each treatment, including control

samples. cDNA was prepared from control and treated samples, labeled and hybridized to HgU133A + 2 human affymetrix DNA microarray. Hybridization, washing, scanning and analysis of genechips were performed at the University of Western Ontario, London Regional Genomics Centre (London, Ontario, Canada).

An average intensity of each E2-treated sample was compared to the average intensity for control non-treated samples. Three biological replicates for each array were processed and the data was transformed using Robust Multi-Array normalization (5) and values below 0.01 were set to 0.01. Each measurement was normalized by dividing all measurements in that sample by the 50th percentile. Ratios were then calculated for all samples against the median of the control samples. A student *t*-test statistical analysis was conducted and false positives were reduced using Benjamini and Hochberg false discovery rate.

4.5. Chromatin immunoprecipitation assay

MCF-7 cells were cross-linked with 1% formaldehyde at room temperature for 5 min. Cross-linking was quenched by immediately washing cells twice with ice-cold PBS and harvesting in PBS containing PMSF. Cell pellets were lysed in 0.2 ml of cell lysis buffer (50 mM Tris–HCl [pH 8.1], 10 mM EDTA, 1% SDS, and protease inhibitors) and incubated on ice for 10 min. Lysates were sonicated to yield DNA fragments ranging in size from 300- to 1000-bp. Approximately 450 μg of the cross-linked, sheared chromatin solution was used for immunoprecipitation. A small portion of each IP was saved as input DNA (5%). Supernatants were diluted 10-fold in dilution buffer (20 mM Tris–HCl [pH 8.1], 1% Triton X-100, 2 mM EDTA, 150 mM NaCl, and protease inhibitors) and immunoprecipitated using a protein A-Sepharose slurry or with MagnaChIP Protein A magnetic beads.

When using the Protein A-Sepharose slurry, lysates were precleared with 50 μl of 50% slurry protein A-Sepharose containing 2.5 μg of sheared salmon sperm DNA for 2 h at 4 °C. Immunoprecipitation was performed overnight at 4 °C with 1.5–4 μg of the antibodies. 50 μl of protein A-Sepharose containing 2.5 μg of salmon sperm DNA per ml was added to the solution and incubated for 1 h at 4 °C. Magnetic beads were washed using PBS with 0.1% Tween-20, incubated with the relevant antibodies for 2.5 h at 4 °C, and rewashed prior to immunoprecipitation overnight at 4 °C. The beads were washed one time each with wash buffer I (0.1% SDS, 1% Triton X-100, 2 mM EDTA, 20 mM Tris–HCl, 150 mM NaCl), wash buffer II (0.1% SDS, 1% Triton X-100, 2 mM EDTA, 20 mM Tris–HCl, 500 mM NaCl), wash buffer III (0.25 M LiCl; 1% NP-40; 1% Na-Deoxycholate; 1 mM EDTA; 10 mM TrisHCl) and twice with TE buffer. Immunoprecipitated material was extracted twice with 150 μl elution buffer (1% SDS-0.1 M $NaHCO_3$). If sequential ChIP was conducted, eluted samples were re-immunoprecipitated overnight at 4 °C with 1.5–4 μg of secondary antibodies. Washes and elution steps were repeated. NaCl was added to the final 150 μl eluate to a concentration of 200 mM and the cross-linking was reversed by heating at 65 °C overnight. DNA was purified using Qiagen PCR purification spin columns.

For analysis by conventional PCR, conditions were as follows: initial denaturing cycle of at 94 °C for 3 min, followed by 40 cycles of 94 °C for 30 s, ~57 °C for 30 s and 72 °C for 45 s, and a final elongation step of 72 °C for 10 min. For experiments involving E2-stimulation, MCF-7 cells were plated to approximately 90% confluence and treated with 10^{-7} M E2 for 45 min prior to ChIP analysis.

For some experiments, DNA isolated from ChIP experiments was subjected to quantitation by real time PCR using Brilliant SYBR green master mix (Stratagene; 600548). Primers were identified using the Primer Express program (Stratagene) and tested to establish optimum reaction conditions. Reactions were performed in a 25 μl volume according to manufacturer's recommendations. The reaction was carried out and measured using Mx3000P realtime instrument. Standard curves were generated using total input DNA (copy number range: 8×10^5 to 8×10^1). The IP and IgG DNA copy number was calculated by extrapolating their respective Ct value from the standard curve. The nonimmune IgG copy number was subtracted from IP DNA copy number. The resulting IP copy number was initially normalized against the total input DNA by dividing the IP by input. The average copy number with E2-treated IPs was then normalized to untreated control IPs, and recruitment represented as a fold-change with E2-treatment. All measurements were done in duplicate and an average Ct value was used to calculate copy number. Two independent realtime reactions were done for each experiment.

4.6. ChIP-DSL assay

Chromatin immunoprecipitation coupled to DNA selection and Ligation (ChIP-DSL) was used to assess global promoter occupancy by p/CIP/CARM1. MCF-7 cells were cross-linked with formaldehyde and subjected to standard sequential ChIP–reChIP assay using affinity purified anti-p/CIP and anti-CARM1 antibodies. The procedure for oligonucleotide annealing, solid phase selection ligation and PCR amplification were performed exactly as described (Aviva Systems Biology; H20K, Cat# AK-0504). The antibody-enriched DNA and the total input were biotinylated followed by annealing to the 40mer oligonucleotide pool. The DNA–oligonucleotide complexes are then selected by binding to streptavidin-conjugated magnetic beads, while the non-annealed oligonucleotides are washed away. Correctly paired 40mers are then ligated to form the corresponding 80mer which is flanked by both universal primer annealing sites (T3 and T7) giving rise to a complete amplicon. A PCR reaction was then conducted on the amplicons using fluorescently labeled T7 and regular T3 primers. Total input DNA was PCR amplified using Cy5 (green) labeled T7 primer and the immunoprecipitated (IP) sample was amplified using Cy3 (red) labeled T7 primer. The PCR products are co-hybridized to the 40mer array (Hu20K) to derive an enrichment ratio for each target. After hybridization and washing, array slides were scanned on a One Virtek (Bio-Rad) Chip Reader, and the ArrayVision (v6.0) software package (London Regional Genomics Centre, London, Ontario, Canada) was used to quantify fluorescence intensity. The Chip on chip intensity values were normalized using a Lowess curve, which was fit to the log intensity versus log-ratio plot and 20% of the data was used to calculate the Lowess fit at each point. Following normalization, a two-sided student's *t*-test was conducted where standard deviation of the replicates was used to calculate a p-value. Fold change was calculated for each gene using a mean value that was calculated from all three biological replicates.

4.7. Ingenuity Pathway Analysis

Ingenuity Pathways Systems (http://www.ingenuity.com) analysis was employed to group statistically significant genes. The 204 genes that bound p/CIP/CARM1 directly and were transcriptionally affected by E2 were considered for Functional Analysis to identify the biological functions and/or diseases that were most significant to the data set. A right-tailed Fisher's exact test was used to calculate a p-value determining the probability that each biological function and/or disease assigned to that data set is due to chance alone.

4.8. Promoter enrichment analysis

Promoter sequences were identified using Gene2Promoter within the Genomatix Suite (www.genomatix.de). Input was in the form of gene accession numbers, and comparison with transcripts that have been mapped to the ElDorado genome yielded mapped sequence results and extracted promoters. A defined 1000 bp upstream of the mapped transcriptional start sites were selected for further transcription factor binding site analysis. To search for enriched consenus motifs within ElDorado extracted promoter sequences the BIOBASE Knowledge Library was used, making use of MATCH software and the Transfac

database. Searches were performed with the best supported promoters using the vertebrate non redundant (minFP) profile. Background frequencies were determined using control set of human housekeeping gene promoters. Optimized matrix cutoffs and search window positions were used. Significant matrices were found with p-value<0.001 and Yes/No>1.2.

Acknowledgements

JT was supported by operating grants from CIHR and NCIC while this work was being conducted. NC was the recipient of an Ontario Graduate Scholarship, a Canadian Institutes for Health Research Strategic Training Scholarship and a Translational Breast Cancer Scholarship through the London Regional Cancer Program, and GT was supported by a CIHR pre-doctoral fellowship.

Appendix A. Supplementary data

Supplementary data to this article can be found online at http://dx.doi.org/10.1016/j.bbamcr.2013.02.009.

References

[1] J. Torchia, C. Glass, M.G. Rosenfeld, Co-activators and co-repressors in the integration of transcriptional responses, Curr. Opin. Cell Biol. 10 (1998) 373–383.
[2] R. Métivier, G. Reid, F. Gannon, Transcription in four dimensions: nuclear receptor-directed initiation of gene expression, EMBO Rep. 7 (2006) 161–167.
[3] R. Métivier, G. Penot, M.R. Hübner, G. Reid, H. Brand, M. Kos, F. Gannon, Estrogen receptor-alpha directs ordered, cyclical, and combinatorial recruitment of cofactors on a natural target promoter, Cell 115 (2003) 751–763.
[4] J. Torchia, D.W. Rose, J. Inostroza, Y. Kamei, S. Westin, C.K. Glass, M.G. Rosenfeld, The transcriptional co-activator p/CIP binds CBP and mediates nuclear-receptor function, Nature 387 (1997) 677–684.
[5] H. Chen, R.J. Lin, R.L. Schiltz, D. Chakravarti, A. Nash, L. Nagy, M.L. Privalsky, Y. Nakatani, R.M. Evans, Nuclear receptor coactivator ACTR is a novel histone acetyltransferase and forms a multimeric activation complex with P/CAF and CBP/p300, Cell 90 (1997) 569–580.
[6] S.L. Anzick, J. Kononen, R.L. Walker, D.O. Azorsa, M.M. Tanner, X.Y. Guan, G. Sauter, O.P. Kallioniemi, J.M. Trent, P.S. Meltzer, AIB1, a steroid receptor coactivator amplified in breast and ovarian cancer, Science 277 (1997) 965.
[7] C.S. Suen, T.J. Berrodin, R. Mastroeni, B.J. Cheskis, C.R. Lyttle, D.E. Frail, A transcriptional coactivator, steroid receptor coactivator-3, selectively augments steroid receptor transcriptional activity, J. Biol. Chem. 273 (1998) 27645–27653.
[8] H. Li, P.J. Gomes, J.D. Chen, RAC3, a steroid/nuclear receptor-associated coactivator that is related to SRC-1 and TIF2, Proc. Natl. Acad. Sci. U. S. A. 94 (1997) 8479–8484.
[9] A. Takeshita, G.R. Cardona, N. Koibuchi, C.S. Suen, W.W. Chin, TRAM-1, a novel 160-kDa thyroid hormone receptor activator molecule, exhibits distinct properties from steroid receptor coactivator-1, J. Biol. Chem. 272 (1997) 27629–27634.
[10] X. Li, D.M. Lonard, S.Y. Jung, A. Malovannaya, Q. Feng, J. Qin, S.Y. Tsai, M.J. Tsai, B.W. O'Malley, The SRC-3/AIB1 coactivator is degraded in a ubiquitin- and ATP-independent manner by the REGgamma proteasome, Cell 124 (2006) 381–392.
[11] L. Liao, S.Q. Kuang, Y. Yuan, S.M. Gonzalez, B.W. O'Malley, J. Xu, Molecular structure and biological function of the cancer-amplified nuclear receptor coactivator SRC-3/AIB1, J. Steroid Biochem. Mol. Biol. 83 (2002) 3–14.
[12] Y. Shang, X. Hu, J. DiRenzo, M.A. Lazar, M. Brown, Cofactor dynamics and sufficiency in estrogen receptor-regulated transcription, Cell 103 (2000) 843–852.
[13] M.D. Planas-Silva, Y. Shang, J.L. Donaher, M. Brown, R.A. Weinberg, AIB1 enhances estrogen-dependent induction of cyclin D1 expression, Cancer Res. 61 (2001) 3858–3862.
[14] M.C. Louie, J.X. Zou, A. Rabinovich, H.W. Chen, ACTR/AIB1 functions as an E2F1 coactivator to promote breast cancer cell proliferation and antiestrogen resistance, Mol. Cell. Biol. 24 (2004) 5157–5171.
[15] R.C. Wu, J. Qin, Y. Hashimoto, J. Wong, J. Xu, S.Y. Tsai, M.J. Tsai, B.W. O'Malley, Regulation of SRC-3 (pCIP/ACTR/AIB-1/RAC-3/TRAM-1) coactivator activity by I kappa B kinase, Mol. Cell. Biol. 22 (2002) 3549–3561.
[16] H. Naeem, D. Cheng, Q. Zhao, C. Underhill, M. Tini, M.T. Bedford, J. Torchia, The activity and stability of the transcriptional coactivator p/CIP/SRC-3 are regulated by CARM1-dependent methylation, Mol. Cell. Biol. 27 (2007) 120–134.
[17] R.W. Li, A.V. Capuco, Canonical pathways and networks regulated by estrogen in the bovine mammary gland, Funct. Integr. Genomics 8 (2008) 55–68.
[18] R.C. Wu, Q. Feng, D.M. Lonard, B.W. O'Malley, SRC-3 coactivator functional lifetime is regulated by a phospho-dependent ubiquitin time clock, Cell 129 (2007) 1125–1140.
[19] R.C. Wu, J. Qin, P. Yi, J. Wong, S.Y. Tsai, M.J. Tsai, B.W. O'Malley, Selective phosphorylations of the SRC-3/AIB1 coactivator integrate genomic responses to multiple cellular signaling pathways, Mol. Cell 15 (2004) 937–949.
[20] H. Wu, L. Sun, Y. Zhang, Y. Chen, B. Shi, R. Li, Y. Wang, J. Liang, D. Fan, G. Wu, D. Wang, S. Li, Y. Shang, Coordinated regulation of AIB1 transcriptional activity by sumoylation and phosphorylation, J. Biol. Chem. 281 (2006) 21848–21856.
[21] H. Ma, C.T. Baumann, H. Li, B.D. Strahl, R. Rice, M.A. Jelinek, D.W. Aswad, C.D. Allis, G.L. Hager, M.R. Stallcup, Hormone-dependent, CARM1-directed, arginine-specific methylation of histone H3 on a steroid-regulated promoter, Curr. Biol. 11 (2001) 1981–1985.
[22] B.T. Schurter, S.S. Koh, D. Chen, G.J. Bunick, J.M. Harp, B.L. Hanson, A. Henschen-Edman, D.R. Mackay, M.R. Stallcup, D.W. Aswad, Methylation of histone H3 by coactivator-associated arginine methyltransferase 1, Biochemistry 40 (2001) 5747–5756.
[23] S. Daujat, U.M. Bauer, V. Shah, B. Turner, S. Berger, T. Kouzarides, Crosstalk between CARM1 methylation and CBP acetylation on histone H3, Curr. Biol. 12 (2002) 2090–2097.
[24] D. Chen, S.M. Huang, M.R. Stallcup, Synergistic, p160 coactivator-dependent enhancement of estrogen receptor function by CARM1 and p300, J. Biol. Chem. 275 (2000) 40810–40816.
[25] Y.H. Lee, S.S. Koh, X. Zhang, X. Cheng, M.R. Stallcup, Synergy among nuclear receptor coactivators: selective requirement for protein methyltransferase and acetyltransferase activities, Mol. Cell. Biol. 22 (2002) 3621–3632.
[26] C. Teyssier, D. Chen, M.R. Stallcup, Requirement for multiple domains of the protein arginine methyltransferase CARM1 in its transcriptional coactivator function, J. Biol. Chem. 277 (2002) 46066–46072.
[27] S. El Messaoudi, E. Fabbrizio, C. Rodriguez, P. Chuchana, L. Fauquier, D. Cheng, C. Theillet, L. Vandel, M.T. Bedford, C. Sardet, Coactivator-associated arginine methyltransferase 1 (CARM1) is a positive regulator of the Cyclin E1 gene, Proc. Natl. Acad. Sci. U. S. A. 103 (2006) 13351–13356.
[28] S. Frietze, M. Lupien, P.A. Silver, M. Brown, CARM1 regulates estrogen-stimulated breast cancer growth through up-regulation of E2F1, Cancer Res. 68 (2008) 301–306.
[29] S.S. Koh, D. Chen, Y.H. Lee, M.R. Stallcup, Synergistic enhancement of nuclear receptor function by p160 coactivators and two coactivators with protein methyltransferase activities, J. Biol. Chem. 276 (2001) 1089–1098.
[30] B.D. Strahl, S.D. Briggs, C.J. Brame, J.A. Caldwell, S.S. Koh, H. Ma, R.G. Cook, J. Shabanowitz, D.F. Hunt, M.R. Stallcup, C.D. Allis, Methylation of histone H4 at arginine 3 occurs in vivo and is mediated by the nuclear receptor coactivator PRMT1, Curr. Biol. 11 (2001) 996–1000.
[31] H. Wang, Z.-Q. Huang, L. Xia, Q. Feng, H. Erdjument-Bromage, B.D. Strahl, S.D. Briggs, C.D. Allis, J. Wong, P. Tempst, Y. Zhang, Methylation of histone H4 at arginine 3 facilitating transcriptional activation by nuclear hormone receptor, Science 293 (2001) 853–857.
[32] I. Garcia-Bassets, Y.S. Kwon, F. Telese, G.G. Prefontaine, K.R. Hutt, C.S. Cheng, B.G. Ju, K.A. Ohgi, J. Wang, L. Escoubet-Lozach, D.W. Rose, C.K. Glass, X.D. Fu, M.G. Rosenfeld, Histone methylation-dependent mechanisms impose ligand dependency for gene activation by nuclear receptors, Cell 128 (2007) 505–518.
[33] J.S. Carroll, C.A. Meyer, J. Song, W. Li, T.R. Geistlinger, J. Eeckhoute, A.S. Brodsky, E.K. Keeton, K.C. Fertuck, G.F. Hall, Q. Wang, S. Bekiranov, V. Sementchenko, E.A. Fox, P.A. Silver, T.R. Gingeras, X.S. Liu, M. Brown, Genome-wide analysis of estrogen receptor binding sites, Nat. Genet. 38 (2006) 1289–1297.
[34] W.J. Welboren, M.A. van Driel, E.M. Janssen-Megens, S.J. van Heeringen, F.C. Sweep, P.N. Span, H.G. Stunnenberg, ChIP-Seq of ERalpha and RNA polymerase II defines genes differentially responding to ligands, EMBO J. 28 (2009) 1418–1428.
[35] M. Boruk, J.G. Savory, R.J. Haché, AF-2-dependent potentiation of CCAAT enhancer binding protein beta-mediated transcriptional activation by glucocorticoid receptor, Mol. Endocrinol. 12 (1998) 1749–1763.
[36] G.G. Préfontaine, R. Walther, W. Giffin, M.E. Lemieux, L. Pope, R.J. Haché, Selective binding of steroid hormone receptors to octamer transcription factors determines transcriptional synergism at the mouse mammary tumor virus promoter, J. Biol. Chem. 274 (1999) 26713–26719.
[37] L. Cicatiello, R. Addeo, A. Sasso, L. Altucci, V.B. Petrizzi, R. Borgo, M. Cancemi, S. Caporali, S. Caristi, C. Scafoglio, D. Teti, F. Bresciani, B. Perillo, A. Weisz, Estrogens and progesterone promote persistent CCND1 gene activation during G1 by inducing transcriptional derepression via c-Jun/c-Fos/estrogen receptor (progesterone receptor) complex assembly to a distal regulatory element and recruitment of cyclin D1 to its own gene promoter, Mol. Cell. Biol. 24 (2004) 7260–7274.
[38] S. Safe, Transcriptional activation of genes by 17 beta-estradiol through estrogen receptor–Sp1 interactions, Vitam. Horm. 62 (2001) 231–252.
[39] S. Safe, K. Kim, Nuclear receptor-mediated transactivation through interaction with Sp proteins, Prog. Nucleic Acid Res. Mol. Biol. 77 (2004) 1–36.
[40] K. Paech, P. Webb, G.G. Kuiper, S. Nilsson, J. Gustafsson, P.J. Kushner, T.S. Scanlan, Differential ligand activation of estrogen receptors ERalpha and ERbeta at AP1 sites, Science 277 (1997) 1508–1510.
[41] P.J. Kushner, D.A. Agard, G.L. Greene, T.S. Scanlan, A.K. Shiau, R.M. Uht, P. Webb, Estrogen receptor pathways to AP-1, J. Steroid Biochem. Mol. Biol. 74 (2000) 311–317.
[42] J.S. Carroll, X.S. Liu, A.S. Brodsky, W. Li, C.A. Meyer, A.J. Szary, J. Eeckhoute, W. Shao, E.V. Hestermann, T.R. Geistlinger, E.A. Fox, P.A. Silver, M. Brown, Chromosome-wide mapping of estrogen receptor binding reveals long-range regulation requiring the forkhead protein FoxA1, Cell 122 (2005) 33–43.
[43] Y.S. Kwon, I. Garcia-Bassets, K.R. Hutt, C.S. Cheng, M. Jin, D. Liu, C. Benner, D. Wang, Z. Ye, M. Bibikova, J.B. Fan, L. Duan, C.K. Glass, M.G. Rosenfeld, X.D. Fu, Sensitive ChIP-DSL technology reveals an extensive estrogen receptor alpha-binding program on human gene promoters, Proc. Natl. Acad. Sci. U. S. A. 104 (2007) 4852–4857.
[44] J. Frasor, J.M. Danes, B. Komm, K.C. Chang, C.R. Lyttle, B.S. Katzenellenbogen, Profiling of estrogen up- and down-regulated gene expression in human breast cancer cells: insights into gene networks and pathways underlying estrogenic control of proliferation and cell phenotype, Endocrinology 144 (2003) 4562–4574.
[45] K. Sakamoto, W.C. Lin, A.A. Triplett, K.U. Wagner, Targeting janus kinase 2 in Her2/neu-expressing mammary cancer: implications for cancer prevention and therapy, Cancer Res. 69 (2009) 6642–6650.

[46] R.J. Sims, D. Reinberg, Histone H3 Lys 4 methylation: caught in a bind? Genes Dev. 20 (2006) 2779–2786.
[47] A.J. Ruthenburg, H. Li, D.J. Patel, C.D. Allis, Multivalent engagement of chromatin modifications by linked binding modules, Nat. Rev. Mol. Cell Biol. 8 (2007) 983–994.
[48] U.M. Bauer, S. Daujat, S.J. Nielsen, K. Nightingale, T. Kouzarides, Methylation at arginine 17 of histone H3 is linked to gene activation, EMBO Rep. 3 (2002) 39–44.
[49] R.B. Lanz, Y. Bulynko, A. Malovannaya, P. Labhart, L. Wang, W. Li, J. Qin, M. Harper, B.W. O'Malley, Global characterization of transcriptional impact of the SRC-3 coregulator, Mol. Endocrinol. 24 (2010) 859–872.
[50] M. Lupien, J. Eeckhoute, C.A. Meyer, S.A. Krum, D.R. Rhodes, X.S. Liu, M. Brown, Coactivator function defines the active estrogen receptor alpha cistrome, Mol. Cell. Biol. 29 (2009) 3413–3423.
[51] K.U. Wagner, H. Rui, Jak2/Stat5 signaling in mammogenesis, breast cancer initiation and progression, J. Mammary Gland Biol. Neoplasia 13 (2008) 93–103.
[52] L. Hennighausen, G.W. Robinson, Interpretation of cytokine signaling through the transcription factors STAT5A and STAT5B, Genes Dev. 22 (2008) 711–721.
[53] A.C. Pfeifer, J. Timmer, U. Klingmüller, Systems biology of JAK/STAT signalling, Essays Biochem. 45 (2008) 109–120.
[54] E.B. Haura, J. Turkson, R. Jove, Mechanisms of disease: insights into the emerging role of signal transducers and activators of transcription in cancer, Nat. Clin. Pract. Oncol. 2 (2005) 315–324.
[55] E. Iavnilovitch, R.D. Cardiff, B. Groner, I. Barash, Deregulation of Stat5 expression and activation causes mammary tumors in transgenic mice, Int. J. Cancer 112 (2004) 607–619.
[56] E. Iavnilovitch, B. Groner, I. Barash, Overexpression and forced activation of stat5 in mammary gland of transgenic mice promotes cellular proliferation, enhances differentiation, and delays postlactational apoptosis, Mol. Cancer Res. 1 (2002) 32–47.
[57] K. Sakamoto, B.A. Creamer, A.A. Triplett, K.U. Wagner, The Janus kinase 2 is required for expression and nuclear accumulation of cyclin D1 in proliferating mammary epithelial cells, Mol. Endocrinol. 21 (2007) 1877–1892.
[58] H. Yamashita, H. Iwase, T. Toyama, Y. Fujii, Naturally occurring dominant-negative Stat5 suppresses transcriptional activity of estrogen receptors and induces apoptosis in T47D breast cancer cells, Oncogene 22 (2003) 1638–1652.
[59] H. Yamashita, M. Nishio, Y. Fujii, H. Iwase, Dominant-negative Stat5 inhibits growth and induces apoptosis in T47D-derived tumors in nude mice, Cancer Sci. 95 (2004) 662–665.
[60] C.M. Silva, M.A. Shupnik, Integration of steroid and growth factor pathways in breast cancer: focus on signal transducers and activators of transcription and their potential role in resistance, Mol. Endocrinol. 21 (2007) 1499–1512.
[61] A. Barski, S. Cuddapah, K. Cui, T.Y. Roh, D.E. Schones, Z. Wang, G. Wei, I. Chepelev, K. Zhao, High-resolution profiling of histone methylations in the human genome, Cell 129 (2007) 823–837.
[62] N.D. Heintzman, R.K. Stuart, G. Hon, Y. Fu, C.W. Ching, R.D. Hawkins, L.O. Barrera, S. Van Calcar, C. Qu, K.A. Ching, W. Wang, Z. Weng, R.D. Green, G.E. Crawford, B. Ren, Distinct and predictive chromatin signatures of transcriptional promoters and enhancers in the human genome, Nat. Genet. 39 (2007) 311–318.